RESONANT TUNNELING CALCULATIONS VIA THE DENSITY MATRIX IN THE COORDINATE REPRESENTATION

H. L. Grubin and T. R. Govindan
Scientific Research Associates, Inc.
PO Box 1058
Glastonbury CT 06033

ABSTRACT

Solutions of the quantum Liouville equation in the coordinate representation, including dissipation, have be implemented for studying the double barrier resonant tunneling diode.

I. INTRODUCTION

Simulations of the quantum Liouville equation in the coordinate representation have been obtained for resonant tunneling structures. The coordinate representation equation includes dissipation represented via a quasi Femi level. The two relevant equations (apart from Poisson's equation) are the equation of motion for the density matrix $\rho(x,x',t)$:

$$(1) \qquad i\hbar\frac{\partial\rho(x,x',t)}{\partial t} = -\frac{\hbar^2}{2m}\left(\frac{\partial^2}{\partial x^2}-\frac{\partial^2}{\partial x'^2}\right)\rho(x,x',t)+\left[(V(x)-V(x'))-(E_F(x)-E_F(x'))\right]\rho(x,x',t)$$

and the equation constraining the quasi-Femi level, the current density j, the position dependent scattering rate, $\Gamma(x)$, and the density $\rho(x)=\rho(x,x)$:

$$(2) \qquad E_F(x)-E_F(x') = -j\int_{x'}^{x}dx''m\Gamma(x'')/\rho(x'')$$

Each of these equations has been discussed in recent publications [1 ,2]. In particular, the algorithm used to solve these equations was discussed in [2]. Recent improvements summarized below have resulted in greater robustness and enable some of the calculations of this paper.

II. THE RESONANT TUNNELING STRUCTURE

The application of equations (1), (2) and Poisson's equation is to resonant tunneling structures. We treat a 200nm structure, with two 5 nm - 300 mev barriers separated by a 5nm well. The structure has a nominal doping of $10^{24}/m^3$ except for a central 50nm wide region where the doping is reduced to $10^{22}/m^3$. The effective mass is constant and equal to that of GaAs ($0.067m_0$); Fermi statistics are imposed; the ambient is 77K; and current is imposed through the density matrix equivalent of a displaced distribution at the boundaries (see [2]).

The signature of the RTD is it's current-voltage relation with the region of negative differential conductivity; for the structure considered this is displayed in figure 1. The current is numerically negligible until a bias of approximately 50 mev, with the peak current occurring at 260 mev, followed by a sharp but modest drop in current at 270 mev. The interpretation of these results is assisted by figures (2) and (3) and the Bohm quantum potential:

$$(3) \qquad Q = -\frac{\hbar^2}{2m} \frac{\partial^2 \sqrt{\rho(x)}}{\sqrt{\rho(x)}\, \partial x^2}$$

We have found, through an extensive number of numerical simulations, that the value of $V(x)+Q(x)$, between the barriers of an RTD is a measure of the position of the quasi-bound state.

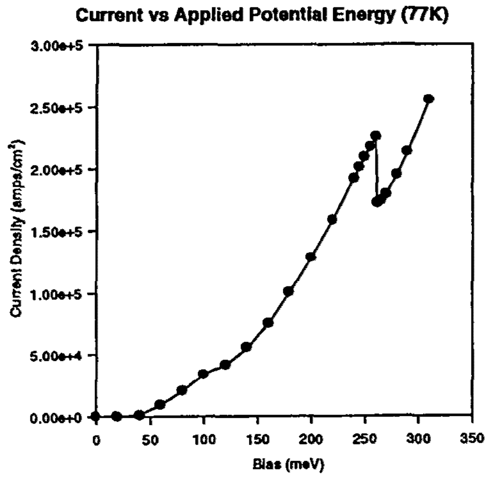

Figure 1. Current versus voltage for the resonant tunneling structure.

Consider figure 2 which displays the equilibrium self-consistent potential for the RTD. Also shown is the value of the equilibrium Fermi energy (approximately 54 mev) and the values, at five different values of applied potential energy, of $V(x)+Q(x)$ within the quantum well. At 100 mev the quasi-bound state is approximately equal to the equilibrium Fermi energy and significant current begins to flow. The current continues to increase until the bias equals 260 mev, where there is a sudden drop in current.

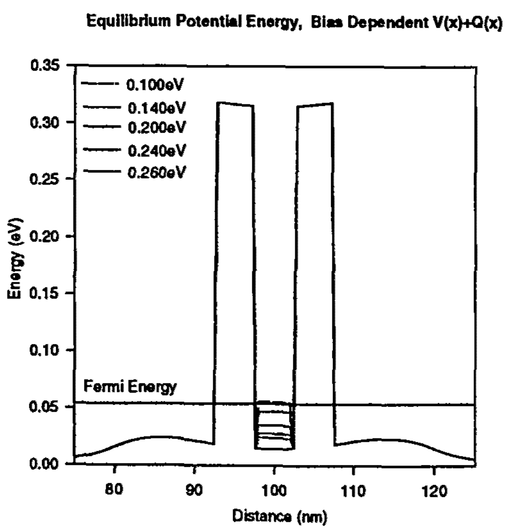

Figure 2. Equilibrium potential energy and the bias dependence of V(x)+Q(x) within the quantum well. Legend denotes collector bias.

To see what is happening we blow up the region on either side of the emitter barrier, where we display values of $V(x)+Q(x)$ before the emitter barrier and within the quantum well (figure 3). Within the quantum well we see the quasi bound state decreasing as the bias on the collector is increasing. In the region prior to the emitter barrier where a 'notch' potential forms signifying charge accumulation, we see the formation with increased bias of a region where $V(x)+Q(x)$ is relatively flat. Of significance here is that for values of bias associated with the initial current increase the value of $V(x)+Q(x)$ within the quantum well is greater then its value in the emitter region. The current reaches a maximum at the cross-over where $V(x)+Q(x)$ in the emitter region and in the quantum well are approximately equal. (Implementation of an earlier algorithm, generally resulted in solutions oscillating between high and low values of current when this condition was reached). While it is tempting to associate $V(x)+Q(x)$ within the emitter region with a quasi-bound state, this association may be premature.

The distribution of potential energy $V(x)$ as a function of bias is displayed in figure 4, where the notch potential is deepened with increasing bias, signifying increased charge accumulation. This is accompanied by a smaller share of the potential drop across the emitter barrier, relative to the collector barrier region. In particular, comparing the slopes of the voltage drop across the emitter and collector barriers, it is apparent that larger fractions of potential energy fall across the collector barrier.

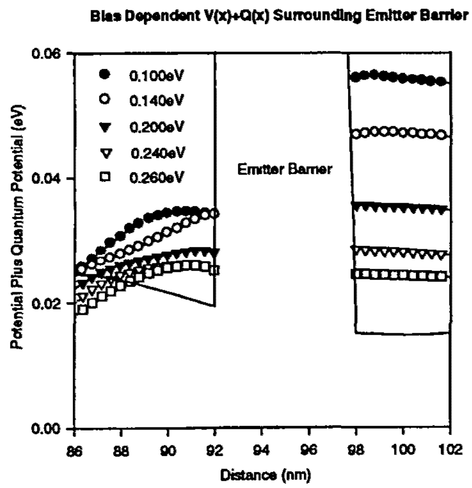

Figure 3. Blow up of figure 2 in the region surrounding the emitter barrier.

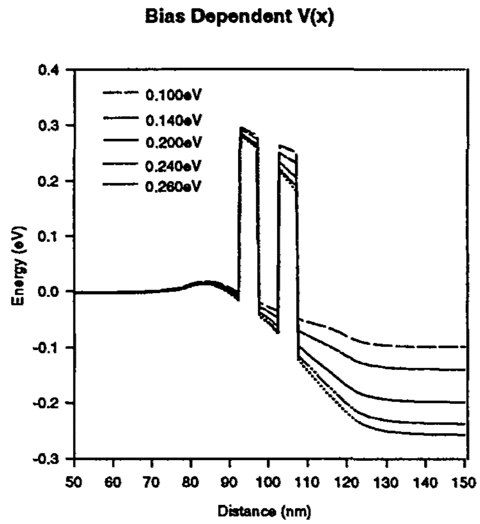

Figure 4. Potential energy V(x) as a function of collector bias

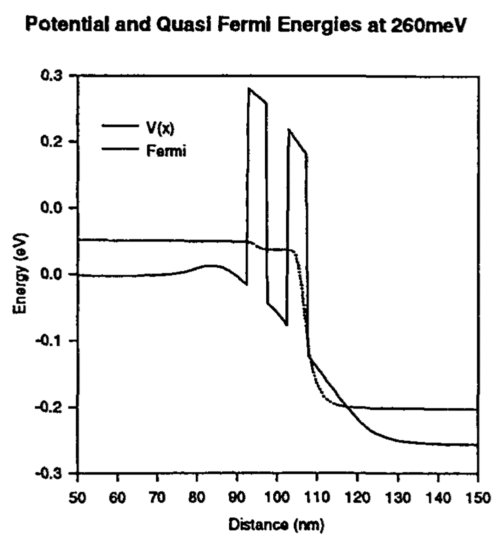

Figure 5 Potential and quasi-Fermi energy at a bias of 260 mev.

Explicit in this calculation is dissipation which is incorporated through the quasi-Fermi level. Within the vicinity of the boundaries the quasi-Fermi level is parallel to the conduction band edge. Indeed, for this calculation the quasi-Fermi level departs from the conduction band edge only within the vicinity of the barriers. The quasi-Fermi level is displayed in figure 5 at a bias of 260 mev, where we see that the quasi-Fermi level is relatively flat until the middle of the first barrier at which point there is a small drop in value followed by a flat region within the quantum well. There is a strong drop of the quasi Fermi level within the second barrier.

The charge distribution accompanying these variations in bias shows accumulation on the emitter side of the barrier along with charge accumulation within the quantum well. The increase in charge within the quantum well and adjacent to the emitter region is accompanying by charge depletion downstream of the second barrier, with the result that the net charge distribution throughout the structure is zero.

In all of the computations associated with figure (1), only one set of scattering rates was used. Variations in the quasi Fermi level were accompanied by variations in density and current which were all obtained in a self-consistent manner. Supplemental computations were performed in which the quasi-Fermi level was varied by altering the scattering rates. The calculations were applied to the post threshold case with values for the scattering rate chosen so to provide a large drop in current. Indeed a current drop by greater than a factor of three was obtained followed by a shallow current increase with increasing bias. The significant difference leading to these changes was the manner in which the quasi-Fermi level changed. Rather than the shallow change depicted in figure 5, there was a larger change in the quasi-Fermi level across the first barrier (figure 6), a result similar to that obtained for single barriers [1].

III COMMENTS ON THE ALGORITHM

The calculations discussed in this paper were obtained from a new solution algorithm that was constructed for the quantum Liouville equation and permits a more convenient specification of boundary conditions, in particular when the device is under bias. The algorithm is based on a reformulation of the governing equations in which a higher order differential equation in the local direction $[(x+x')/2]$ is constructed from the quantum Liouville equation. The reformulated equation behaves like an elliptical equation in the local direction rather than the hyperbolic behavior of the quantum Liouville equation. With appropriate boundary conditions, solutions to the two forms of the quantum Liouville equations are equivalent. However the reformulated equation allows construction of a more robust algorithm that provides desired solution behavior at the contacts by boundary condition specification at both contacts.

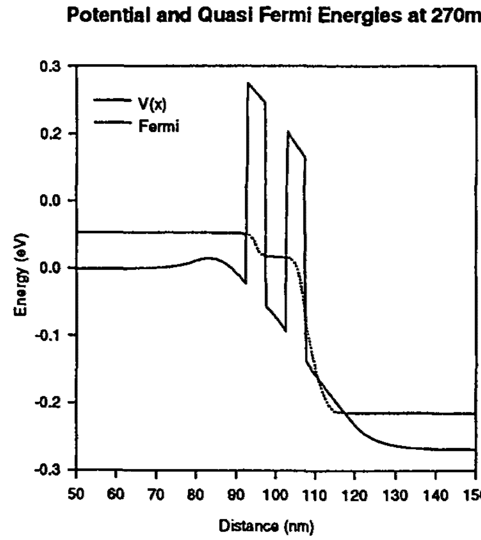

Figure 6. As in figure 5 but for enhanced scattering.

IV SUMMARY

The Liouville equation in the coordinate representation has been implemented for studying resonant tunneling structures. The results provide the first explicit relationship between the range of bias prior to the drop in current and the movement of the quasi-bound states. Additionally, the results provide the first explicit connection between quasi-Fermi levels and the magnitude of the peak to valley ratio in RTDs, and provide evidence that the behavior of RTDs is strongly controlled by dissipation.

V. ACKNOWLEDGMENT

This authors are grateful for the support of ONR and ARO.

VI. REFERENCES

1. H. L. Grubin, T. R. Govindan and M.A. Stroscio, *Semicond. Sci. Technol.* To be published (1994); and D. K. Ferry and H. L. Grubin, To be published in *Solid State Physics*, (H. Ehrenreich, ed) (1994).

2. H. L. Grubin, T. R. Govindan , J. P. Kreskovsky and M. A.Stroscio, *Solid State Electronics* **36**, 1697(1993).